23rd ABCM International Congress of Mechanical Engineering
December 6-11, 2015, Rio de Janeiro, RJ, Brazil

BOUNDS FOR CRACK GROWTH

Cláudio Roberto Ávila da Silva Júnior
Rodrigo Villaca Santos
NuMAT/PPGEM, Federal Technological University of Parana; Av. Sete de Setembro, 3165, Curitiba, PR, Brazil.
DAMEC, Federal Technological University of Parana; Via do Conhecimento, Km 1, Pato Branco, PR, Brazil.
avila@utfpr.edu.br
rodrigov@utfpr.edu.br

Lucas Gimenis de Moura
NuMAT/PPGEM, Federal Technological University of Parana; Av. Sete de Setembro, 3165, Curitiba, PR, Brazil.
falelucas@live.com

Waldir Mariano Machado Júnior
NuMAT/PPGEM, Federal Technological University of Parana; Av. Sete de Setembro, 3165, Curitiba, PR, Brazil.
waldir.jr@pr.senai.br

Abstract. *Linear Elastic Fracture Mechanics (LEFM) describes the propagation of a crack exists in a material, and this propagation is proportional to the range of the stress intensity factor. In the LEFM there are several models that describe the evolution of an initial crack, as the models of Paris-Erdogan and Forman, that are formulated and solved by the determination of an Initial Value Problem (IVP). To few practical applications, it is possible to obtain an exact solution of the IVP. And, in most applications, approximate numerical solutions are used, which can reflect on aspects such as the time and the computational cost. Therefore, the objective of this work is to propose upper and lower bounds for the crack size function for Paris-Erdogan and Forman models. These bounds were determined by the second-order Taylor expansion with Lagrange's rest. Verification of the potentiality of the proposal of this work was accomplished through two numerical examples, and it was observed that for both models was obtained precision and efficiency in the results obtained.*

Keywords: *Linear elastic fracture mechanics, Crack, Initial value problem, Bounds*

1. INTRODUCTION

Fatigue is one of the forms of mechanical failure under a variable loads request whose main feature is the initiation and the propagation of a crack. Linear Elastic Fracture Mechanics (LEFM) is one of the methods for the prediction of life under fatigue, and its proposal describe the propagation of an initial crack in the material.

On LEFM, the propagation of a crack is proportional to the range of the stress intensity factor. Stress intensity factor is a function of parameters such as the load applied, $\Delta\sigma$, the geometry of the material, the crack size and the function of stress intensity factor correction, $f(.)$. In this method, there are several models of crack propagation, with various approaches and conceptions, as highlighted in his works the authors Toor (1973), Hoeppner and Krupp (1974), Beden et al. (2009) and Schijve (2009). Specifically, a distinction is made between the crack propagation models under constant or variable amplitude loads. For the constant amplitude loads models, include models of Paris-Erdogan (1961; 1963), Forman (1967; 1972), Walker (1970), among others. The formulation and solution of these models are based on the determination of an Initial Value Problem (IVP), which describes the evolution of an initial crack. To few practical applications, it is possible to obtain an exact solution of the IVP. In general, in most applications approximate numerical solutions are used, which can reflect on aspects such as the time and the computational cost.

The objective of this work is to propose functions that will be upper and lower bounds to describe the behavior of an initial crack, improving the way of obtaining the results. These bounds will be developed from the models of Paris-Erdogan and Forman, and upper and lower bounds will be the exact solution or numerical solution of the IVP. The development of these bounds will be determined by the second-order Taylor expansion with Lagrange's rest. And for the validation of this work, the comparison will be made of the upper and lower bounds and the approximate numerical solution using the fouth-order Runge-Kutta method (RK4) (ASCHER, PETZOLD, 1998) for two numerical examples.

2. METHOD

Upper and lower bounds for the models of Paris-Erdogan and Forman were developed from the second-order Taylor expansion with Lagrange's rest applied to IVP of each model. For that, they were required to establish hypotheses regarding: the models used, $\left[\left(da/dN\right)\left(N\right)\right]$, loading applied, $\Delta\sigma$, and to the function of stress intensity factor correction, $f(.)$. With respect to models, the IVP for model of Paris-Erdogan is:

$$\begin{cases} \text{Find } a \in C^1\left[\left(N_o, N_1\right); \mathbb{R}^+\right], \text{such that :} \\ \left(\dfrac{da}{dN}\right)\left(N\right) = C_P\left(\sqrt{\Pi a\left(N\right)}\, f\left(a\left(N\right)\right)\Delta\sigma\right)^{m_P}, \forall N \in \left(N_o, N_1\right); \\ a\left(N_o\right) = a_o, \end{cases} \tag{1}$$

where C_p e m_p are material constant and N represents number of load cycles. And, the IVP for model of Forman is:

$$\begin{cases} \text{Find } a \in C^1\left[\left(N_o, N_1\right); \mathbb{R}^+\right], \text{such that :} \\ \left(\dfrac{da}{dN}\right)\left(N\right) = \dfrac{C_F\left(\sqrt{\Pi a\left(N\right)}\, f\left(a\left(N\right)\right)\Delta\sigma\right)^{m_F}}{\left(1-R\right)K_c - \Delta K}, \forall N \in \left(N_o, N_1\right); \\ a\left(N_o\right) = a_o. \end{cases} \tag{2}$$

where C_F e m_F are material constant and N represents number of load cycles. The hypotheses for the models require that the derivate of $a(.)$, crack size, is a function continues and a_0, initial crack size, be known. The hypotheses for loading applied, $\Delta\sigma$, and to the function of stress intensity factor correction, $f(.)$, are:

$$\begin{aligned} &\text{H1}: \Delta\sigma\left(N\right) = \Delta\sigma_0, \forall N \in \left[N_0, N_1\right]; \\ &\text{H2}: \begin{cases} f \in C^1\left(\left[a_0, a_1\right]; \mathbb{R}^+ \setminus \{0\}\right); \\ 0 < f\left(a_0\right) \le f\left(x\right) \le f\left(y\right), x \le y, \forall\, x, y \in \left[a_0, a_1\right]; \\ f'\left(a_0\right) \le f'\left(x\right) \le f'\left(y\right), x \le y, \forall\, x, y \in \left[a_0, a_1\right]; \end{cases} \\ &\text{H3}: \begin{cases} m_P \ge 2; \\ m_F \ge 1. \end{cases} \end{aligned} \tag{3}$$

where $a_0 = a\left(N_0\right)$ e $a_1 = a\left(N_1\right)$. Hypotheses (H1) assumes constant loading. Hypothesis (H2) states that the function of stress intensity factor correction must be a monotonously non-decreasing function, and that its derivative must also be a monotonously non-decreasing function. These conditions are met for most common function of stress intensity factor correction, since they represent an intrinsic characteristic of the crack propagation problem. And the hypothesis (H3) sets the value for the constant model of the material. Hypotheses (H1), (H2) and (H3) form the basis for the development of upper and lower bounds for the crack size function.

Equations (1) and (2) are IVP's, defined by an ordinary, first order, non-linear autonomous differential equations. More generally, Eqs. (1) and (2) can be classified as a Cauchy problem, which consist in finding the trajectories which satisfy the IVP differential equation and the initial value, $a_0 = a\left(N_0\right)$.

Thereby, through the second-order Taylor expansion with Lagrange's rest, the functions that define the upper and lower bounds for the model of Paris-Erdogan are:

$$\begin{cases} a\left(N\right) - a_o \le C_P\left\{\left(\Delta K\left(a_0\right)\right)^{m_P} + \left(\dfrac{m_P C_P}{2}\right)\left(\Delta K\left(a^*\right)\right)^{2m_P}\left[\dfrac{1}{2a^*} + \left(\dfrac{f'}{f}\right)\left(a^*\right)\right]\left(N - N_o\right)\right\}\left(N - N_o\right); \\ a\left(N\right) - a_o \ge C_P\left(\Delta K\left(a_0\right)\right)^{m_P}\left\{1 + \left(\dfrac{m_P C_P}{2}\right)\left(\Delta K\left(a_o\right)\right)^{m_P}\left[\dfrac{1}{2a_o} + \left(\dfrac{f'}{f}\right)\left(a_0\right)\right]\left(N - N_o\right)\right\}\left(N - N_o\right); \\ \forall N \in \left[N - N_o\right]. \end{cases} \tag{4}$$

And for the model of Forman, through the second-order Taylor expansion with Lagrange's rest, the functions that define the upper and lower bounds are:

$$\begin{cases} a(N)-a_o \leq \left\{ \begin{array}{l} \dfrac{C_F\left(\Delta K\left(a_0\right)\right)^{m_F}}{\left(1-R\right)K_c-\Delta K\left(a_0\right)}+\dfrac{1}{2}\left[\dfrac{C_F\left(\Delta K\left(a^*\right)\right)^{m_F}}{\left(1-R\right)K_c-\Delta K\left(a^*\right)}\right]^2\left[m_F+\dfrac{1}{\left(1-R\right)\dfrac{K_c}{\Delta K\left(a^*\right)}-1}\right] \\ x\left[\dfrac{1}{2a^*}+\left(\dfrac{f'}{f}\right)\left(a^*\right)\right]\left(N-N_o\right) \end{array} \right\}\left(N-N_o\right); \\ a(N)-a_o \geq \dfrac{C_F\left(\Delta K\left(a_0\right)\right)^{m_F}}{\left(1-R\right)K_c-\Delta K\left(a_0\right)}\left\{ \begin{array}{l} 1+\dfrac{1}{2}\left[\dfrac{C_F\left(\Delta K\left(a_0\right)\right)^{m_F}}{\left(1-R\right)K_c-\Delta K\left(a_0\right)}\right]\left[m_F+\dfrac{1}{\left(1-R\right)\dfrac{K_c}{\Delta K\left(a_0\right)}-1}\right] \\ x\left[\dfrac{1}{2a_0}+\left(\dfrac{f'}{f}\right)\left(a_0\right)\right]\left(N-N_o\right) \end{array} \right\}\left(N-N_o\right); \end{cases} \tag{5}$$
$$\forall N \in \left[N-N_o\right].$$

The upper and lower bounds crack size functions, Eqs. (4) and (5), are second-degree polynomials in the number of cycles (*N*), and are defined as follows:

$$\begin{cases} a_{UB}\left(N\right)=\gamma.N^2+\beta.N+a_o; \\ a_{LB}\left(N\right)=\alpha.N^2+\beta.N+a_o, \forall N \in \left[N_0,N\right]. \end{cases} \tag{6}$$

3. NUMERICAL EXAMPLES

In order to verifying the potentiality of this work, upper and lower bounds of each model were evaluated by means of two numerical examples:

a. Example 1: Finite width plate with center crack.

The example 1 represents a finite plate, with width *b*, and a center crack, a_o, as shown in Fig. 1a. For this example, the function of stress intensity factor correction is (BANNANTINE et al., 1989):

$$f\left(a\left(N\right)\right)=\sqrt{sec\left(\frac{\Pi a\left(N\right)}{2b}\right)}. \tag{7}$$

b. Example 2: Finite plate with a single edge crack.

The example 2 represents a finite plate, with width *b*, and a single edge crack, a_o, as shown in Fig 1b. For this example, the function of stress intensity factor correction is (BANNANTINE et al., 1989):

$$f\left(a\left(N\right)\right)=1.122-0.231\left(\frac{a\left(N\right)}{b}\right)+10.55\left(\frac{a\left(N\right)}{b}\right)^2-21.72\left(\frac{a\left(N\right)}{b}\right)^3+30.39\left(\frac{a\left(N\right)}{b}\right)^4. \tag{8}$$

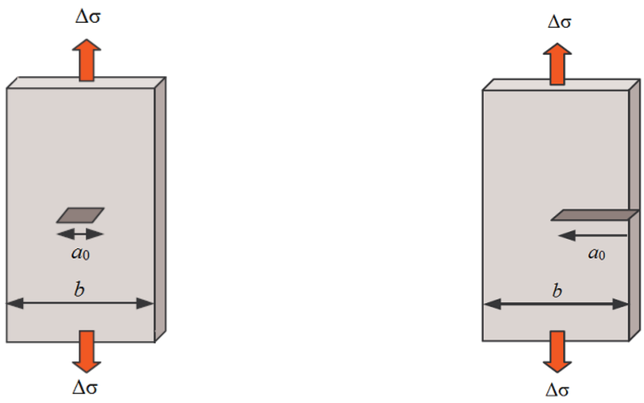

a) **b)**

Figure 1: Fig. a - example 1 - finite width plate with center crack. Fig. b - example 2 - finite plate with a single edge crack.

For the resolution of the numerical examples were defined the parameters used in the equation of each model, as shown Tab. 1. As each model uses in their different equations parameters, in this study were used the same parameters employed in the works of Barsom and Rolf (1999) and Castro and Meggiolaro (2009). These works are applied to ferritic steels, for values of stress ratio (*R*) equal to zero.

Table 1: Parameters that adjust the models of crack propagation for ferritic steels.

Properties – Ferritic Steels: K_C = 250 MPa.m$^{1/2}$, ΔK_{th} = 7 MPa.m$^{1/2}$			
Model	**C (m/ciclo)**	**m**	**R**
Paris-Erdogan	$6.9\text{x}10^{-12}$	3.0	-
Forman	$2\text{x}10^{-9}$	2.9	0

Notes on Eqs. (4) and (5) that the upper bound is a function of the parameter a^* (crack size). Thus, it was used in this work, a specific value for each model that best fits in the representation of crack propagation curves. The value of a^* used was $a^* = \alpha a_0$, where α a constant. In general, two considerations were made to the definition of a^*: the upper bound has a maximum deviation of 5% compared to approximate numerical solution, and that a^* used to be the same in each model, for the two examples applied.

3.1 Evaluation of the results

The results will be presented through a comparison between approximate numerical solution using the RK4 method, and bounds through the following relationships: graphics representing the number of cycles (*N*) and the crack size (*a*), the percentage of the relative deviation of the upper and lower bounds, defined by Eq. (9), and the reason of computing time.

$$\varepsilon_{UB,LB}\left(N_k\right) = \left(\frac{a_{UB,LB}\left(N_k\right) - a_{RK4}\left(N_k\right)}{a_{RK4}\left(N_k\right)}\right) 100\left[\%\right], \forall N_k \in \left\{0,1,\ldots,\mathrm{N}\right\}. \tag{9}$$

For the resolution of the two examples, first, was defined the value of the upper bound $\left(a^*\right)$ valid for both examples. Through graphs *N* x *a*, Figs. 2 and 3, it is observed the variation of the upper bound (a^* with values of $1.2a_0$, $1.3a_0$ and $1.5a_0$) in relation to the RK4 method for models of Paris-Erdogan and Forman, respectively. In example 1, Figs. 2a and 3a, for both models, the value that most closely matches the RK4 is when $a^* = 1.2a_0$. However, in example 2, Figs. 2b and 3b, also for both models, this same value of a^* is no longer a upper bound. Thus, the value of a^* is valid for both examples and models is when $a^* = 1.3a_0$.

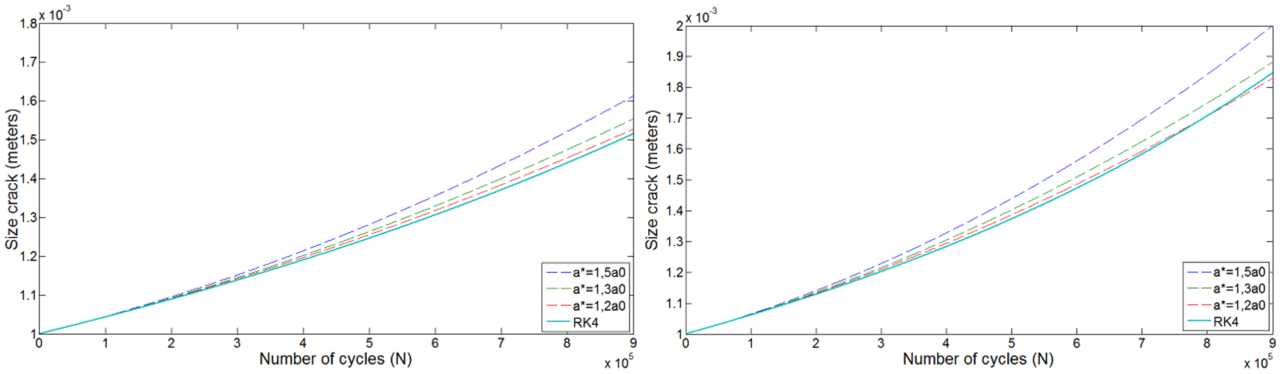

a) b)

Figure 2: Variations of the upper bound (*a with values of 1.2a_o, 1.3a_o and 1.5a_o) in relation the RK4, applied to the examples 1 and 2, Figs. a and b, respectively, for the model of Paris-Erdogan.**

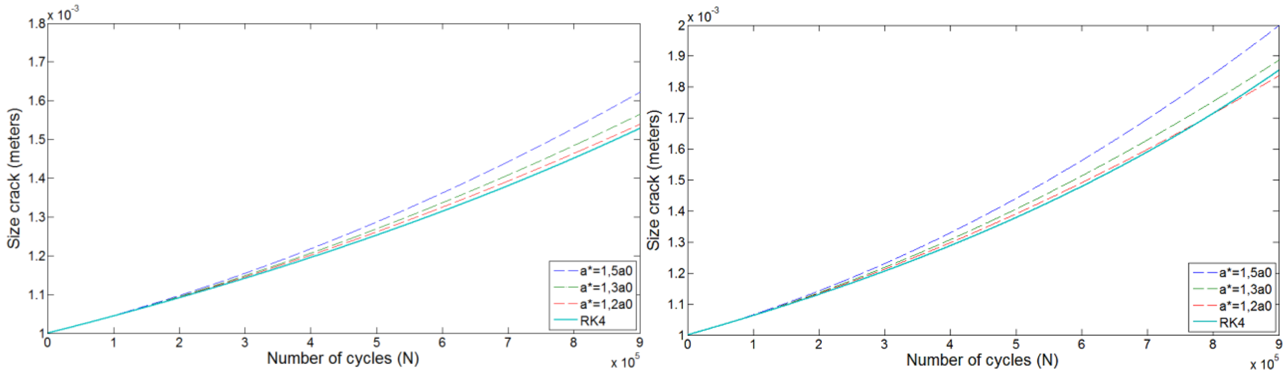

a) b)

Figure 3: Variations of the upper bound (*a with values of 1.2a_o, 1.3a_o and 1.5a_o) in relation the RK4, applied to the examples 1 and 2, Figs. a and b, respectively, for the model of Forman.**

After the definition of upper bound, it was verified the behavior of bounds for the models of Paris-Erdogan and Forman. For the examples were used the following data: loading $\Delta\sigma$ = 70 MPa, number of cycles, N, between 0 to 900000 cycles, initial crack size a = 1 mm and plate width b = 100 mm. Therefore, the Figs. 4 and 5 show through graphics N x a, for models of Paris-Erdogan and Forman, respectively, the crack growth through the solution defined by upper and lower bounds in relation to approximate numerical solution calculated by the RK4 method.

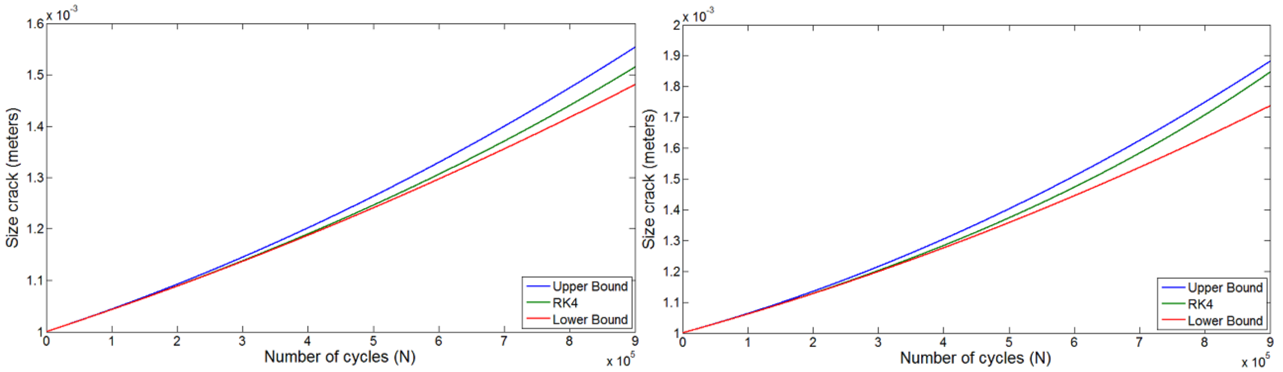

a) b)

Figure 4: Upper and lower bounds and the approximate numerical solution, in relation to the RK4 method for examples 1 and 2, Figs. a and b, respectively, of the Paris-Erdogan model.

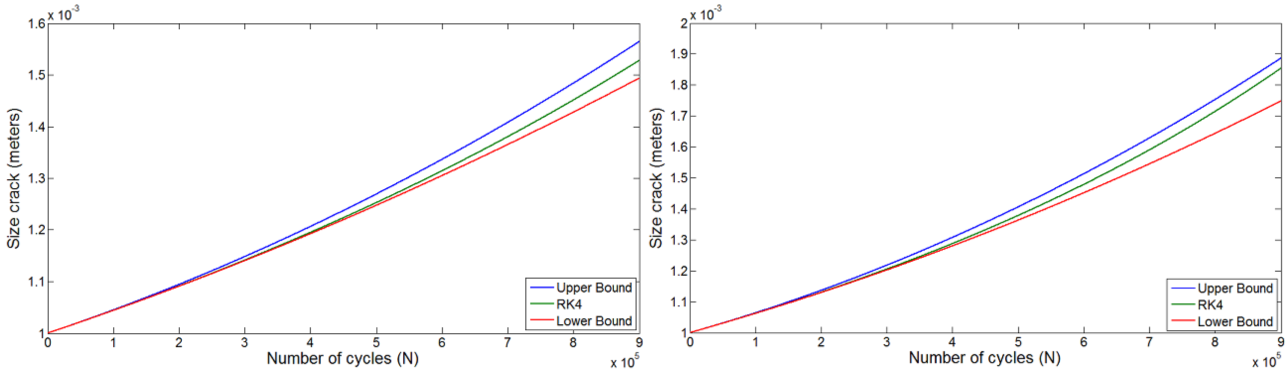

a) **b)**

Figure 5: Upper and lower bounds and the approximate numerical solution, in relation to the RK4 method for examples 1 and 2, Figs. a and b, respectively, of the Forman model.

Thus, through the Figs. 4 and 5, it is observed that the upper and lower bounds are very narrow for models of Paris-Erdogan and Forman in relation to the RK4 method.

As described previously, upper and lower bounds can be written through a second-degree polynomials, according to Eq. (6). Thus, the coefficients of this polynomial, for examples 1 and 2, can be verified according to Tab. 2.

Table 2: Coefficients of the polynomial of Eq. (6) for the examples 1 and 2, applied to models of Paris-Erdogan and Forman.

Paris-Erdogan Model			
Examples	**γ**	**α**	**β**
1	2.20224249129338e-16	1.30288018519031e-16	4.16742725661727e-10
2	4.36541034880858e-16	2.57978645279117e-16	5.86629033180576e-10
Forman Model			
Examples	**γ**	**α**	**β**
1	2.21257464064954e-16	1.33674738809357e-16	4.2816531510184e-10
2	4.30927438837268e-16	2.59892738020747e-16	5.97026915762707e-10

To evaluate the performance of the proposal has been determined the percentage of the relative deviation between bounds in relation to the RK4 method according to Eq. (9). And, after, was given the computational efficiency that is defined by the ratio of the RK4 elapsed time and the bounds elapsed time.

Therefore, for the examples 1 and 2, Figs. 6 and 7, presented in a graph N x *relative deviation*, the percentages of the relative deviation of the upper and lower bounds in relation to the RK4 method for models of Paris-Erdogan and Forman, respectively.

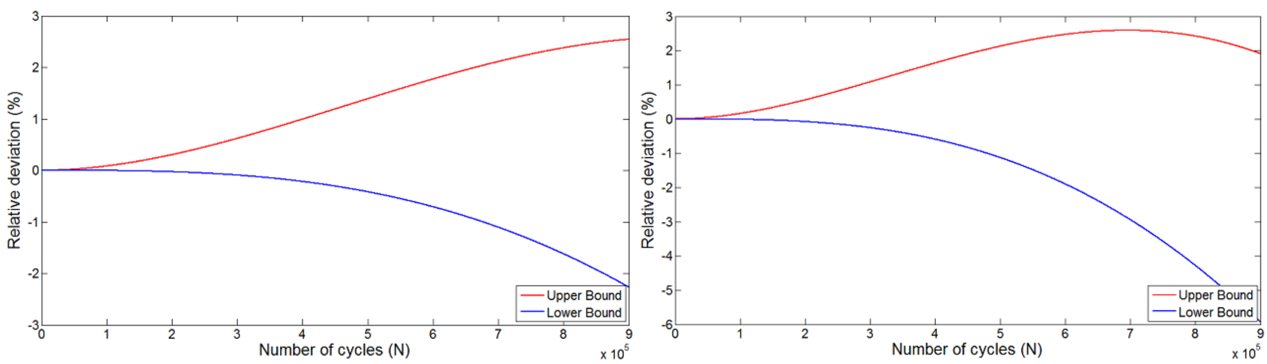

a) **b)**

Figure 6: Percentage of the relative deviation for upper and lower bounds in relation to the RK4 method for examples 1 and 2, Figs. a and b, respectively, of the Paris-Erdogan model.

In Fig. 6a it is observed that the maximum relative deviation for the upper bound corresponds to approximately 2.54% and to lower bound corresponds to approximately -2.27%. And in Fig. 6b verifies that the maximum relative deviation for the upper bound corresponds to approximately 2.59% and for the lower bound the minimum value corresponds to approximately -5.92%.

Thereby, it turns out in Fig. 6a, which for example 1, the relative deviation of the upper and lower bounds are similar, being the lower bound is more accurate than the upper bound each cycle number. And in the example 2, Fig. 6b, the lower bound is more accurate than the upper bound to 600000 cycles. Thus, in general, it turns out that both bounds are accurate in terms of approximation of the RK4 method, because the largest relative deviation observed was -5.92% when N = 900000 cycles for example 2. This value corresponds to a crack size calculated by the RK4 method of 1.85 mm and calculated by the lower bound 1.74 mm.

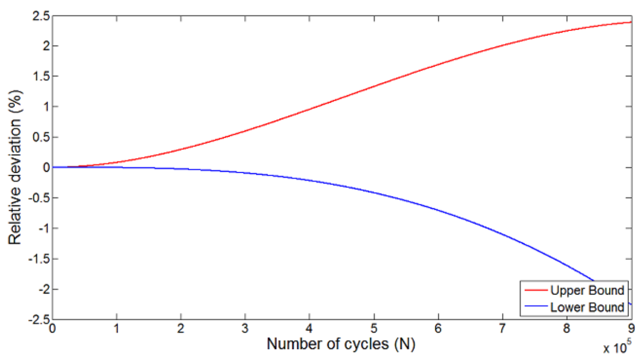

a)

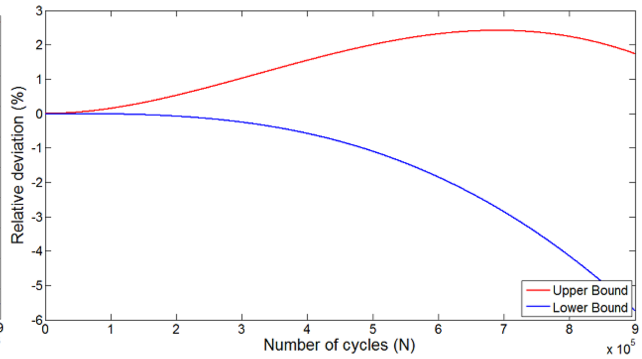

b)

Figure 7: Percentage of the relative deviation for upper and lower bounds in relation to the RK4 method for examples 1 and 2, Figs. a and b, respectively, of the Forman model.

In Fig. 7a shows that the maximum value of the deviation relative to the upper bound corresponds to approximately 2.39% and to lower bound corresponds to approximately -2.26%. In Fig. 7b verifies that the maximum relative deviation for the upper bound corresponds to approximately 2.42% and to lower bound corresponds to approximately -5.73%.

Thereby, it turns out in Fig. 7a, which for example 1, the relative deviation of the upper and lower bounds are similar, being the lower bound is more accurate than the upper bound each cycle number. And in the example 2, Fig. 7b, the lower bound is more accurate than the upper bound to 600000 cycles. Thus, in general, it turns out that both bounds are accurate in terms of approximation of the RK4 method, because the largest relative deviation observed was -5.92% when N = 900000 cycles for example 2. This value corresponds to a crack size calculated by the RK4 method of 1.85 mm and calculated by the lower bound 1.75 mm.

Finally, Tab. 3 shows the approximate elapsed time of the RK4 method and upper and lower bounds to 900000 cycles for models of Paris-Edogan and Forman. For example 1, bounds are 156 and 190 times more computationally efficient compared with the RK4, and for example 2, are 239 and 286 times more efficient computationally than the RK4 for models of Paris-Erdogan and Forman, respectively.

Table 3: Approximate elapsed time (in seconds) of bounds and of the RK4, applied to models of Paris-Erdogan and Forman, to 900000 cycles.

Paris-Erdogan Model			
Examples	**RK4 (sec)**	**Upper / Lower Bounds (sec)**	**Computationally Efficient (ratio of RK4/Bounds)**
1	3.0695	0.0197	**156**
2	4.8829	0.0204	**239**
Forman Model			
Examples	**RK4 (sec)**	**Upper / Lower Bounds (sec)**	**Computationally Efficient (ratio of RK4/Bounds)**
1	3.8494	0.0203	**190**
2	5.5767	0.0195	**286**

4. CONCLUSION

This work introduced an efficient and accurate way to get the evolution of initial crack for models Paris-Erdogan and Forman. Thus, were proposed two functions that are upper and lower bounds for the approximate numerical solution of each model. And for the development of the bounds was necessary a set of hypotheses for each model and the use of the second-order Taylor expansion with Lagrange's rest.

In order to verify the potentiality of the study, two numerical examples were analyzed through a comparison between the bounds and the fouth-order Runge-Kutta method (RK4) by means of the following relationships: graphics representing the number of cycles (N) and the crack size (a), the percentage of the relative deviation of the upper and lower bounds and the reason of computing time.

In general, the performance of bounds regarding the RK4 it was verified in the graphics (N) versus (a) and through the relative deviations. And it was observed that for both models that the study is valid as a way of approximating the behavior of the evolution of the crack. In both examples precision was obtained on the behaviour of bounds as well, were obtained low values of deviations relative. Also, with respect to the computational time, in both models, it was observed that with the use of bounds has been a dynamic monitoring of results.

5. REFERENCES

Ascher, U. M. and Petzold, L. R., 1998. *Computer methods for ordinary differential equations and differential-algebraic equations*. Philadelphia: SIAM.

Bannantine, J. A. et al., 1989. *Fundamentals of metal fatigue analysis*. New Jersey: Prentice Hall, 1st edition.

Barsom J. M. and Rolfe S. T., 1999. *Fracture and fatigue control in structures: Applications of fracture mechanics*. Philadelphia: ASTM, 3rd edition.

Beden, S. M., Abdullah, S. and Ariffin, A. K., 2009. "Review of fatigue crack propagation models for metallic components". *European Journal of Scientific Research*. Vol. 28, n. 3, p. 364-397.

Castro, J. T. P. and Meggiolaro, M .A., 2009. *Fadiga – Técnicas e práticas de dimensionamento estrutural sob cargas reais de serviço*. Create Space, 1st edition.

Forman R. G., Kearney V. E. and Engle R. M., 1967. "Numerical analysis of crack propagation in cyclic-loaded structures". *Journal of Fluids Engineering*. Vol. 89, p. 459-463.

Forman, R. G., 1972. "Study of fatigue crack initiation from flaws using fracture mechanics theory". *Engineering Fracture Mechanics*. Vol. 4, p. 333-345.

Hoeppner, D. W. and Krupp W. E., 1974. "Prediction of component life by application of fatigue crack growth knowledge". *Engineering Fracture Mechanics*. Vol. 6, p. 47-70.

Paris, P. C., Gomez, M. P. and Anderson, W. E., 1961. "A rational analytic theory of fatigue". *The Trend in Engineering*. Vol. 13, p. 9-14.

Paris, P. and Erdogan, F., 1963. "A critical analysis of crack propagation laws". *Journal of Fluids Engineering*. Vol. 85, p. 528-533.

Schijve, J. *Fatigue of structures and materials*. Spinger, 2009, 2nd edition.

Toor, P. M., 1973. "A review of some damage tolerance design approaches for aircraft structures". *Engineering Fracture Mechanics*. Vol. 5, p. 837-880.

Walker, K., 1970. "The effect of stress ratio during crack propagation and fatigue for 2024-T3 and 7076-T6 aluminum. Effect of environment and complex load history on fatigue life". *American Society for Testing and Materials*. p. 1–14.

6. RESPONSIBILITY NOTICE

The authors are the only responsible for the printed material included in this paper.